

Technical Report

Title: *Supplementary Uniaxial Compressive Strength Testing of DGR-3 and DGR-4 Core*

Document ID: TR-08-39


Authors: B. Gorski, T. Anderson and D. Rodgers
CANMET Mining and Mineral Sciences
Laboratories, Natural Resources Canada

Revision: 1

Date: June 18, 2010

DGR Site Characterization Document
Intera Engineering Project 08-200



Intera Engineering DGR Site Characterization Document		
Title:	Supplementary Uniaxial Compressive Strength Testing of DGR-3 and DGR-4 Core	
Document ID:	TR-08-39	
Revision Number:	1	Date: June 18, 2010
Authors:	B. Gorski, T. Anderson and D. Rogers CANMET Mining and Mineral Sciences Laboratories Natural Resources Canada	
Technical Review:	Kenneth Raven, Dougal McCreath, Tom Lam (NWMO)	
QA Review:	John Avis	
Approved by:	 Kenneth Raven	

Document Revision History		
Revision	Effective Date	Description of Changes
0	October 22, 2009	Initial release
1	June 18, 2010	Minor revisions to address NWMO editorial comments of June 15, 2010. Updating of references.

TABLE OF CONTENTS

1	INTRODUCTION	1
2	STANDARD OPERATING PROCEDURES	1
3	SPECIMENS.....	1
4	TEST APPARATUS AND PROCEDURES.....	2
	4.1 Zero Pressure Velocity Tests	2
	4.2 Uniaxial Compression Strength Tests	2
5	ANALYSIS OF DATA.....	2
	5.1 Zero Pressure Velocity Tests	2
	5.2 Uniaxial Compression Strength Tests	3
6	RESULTS AND CONCLUSIONS	5
7	DATA QUALITY AND USE	5
8	DISCLAIMER.....	6
9	REFERENCES	6

LIST OF APPENDICES

APPENDIX A	Data and Calculation Tables
APPENDIX B	Stress-Strain Curves of Tests
APPENDIX C	Specimen Photographs (Before and After Tests)

1 Introduction

Intera Engineering Ltd. has been contracted by the Nuclear Waste Management Organization (NWMO) on behalf of Ontario Power Generation to implement the Geoscientific Site Characterization Plan (GSCP) for the Bruce nuclear site located near Tiverton, Ontario. The purpose of this site characterization work is to assess the suitability of the Bruce site to construct a Deep Geologic Repository (DGR) to store low- and intermediate-level radioactive waste. The GSCP is described by Intera Engineering Ltd. (2006, 2008a).

This Technical Report summarizes the results of supplementary laboratory uniaxial compressive strength testing of core obtained from two deep bedrock boreholes (DGR-3 and DGR-4) as part of Phase 2A of the GSCP.

Natural Resources Canada (NRCan) through the CANMET Mining and Mineral Sciences Laboratories (CANMET-MMSL) was contracted by Intera Engineering Ltd. to provide laboratory geomechanical services. The overall objective of this contract was to determine the physical and mechanical properties of rock core originating from boreholes DGR-1 to DGR-4. This Technical Report describes the test apparatus and procedures and presents the final results of the uniaxial compressive strength tests completed on 11 rock cores. These uniaxial compressive strength test results supplement other earlier geomechanical strength tests reported under separate cover (Intera Engineering Ltd., 2010).

Work described in this Technical Report (TR) was completed in accordance with Intera Test Plan TP-08-12 – Geomechanical Lab Testing of DGR-3 & DGR-4 Core (Intera Engineering Ltd., 2008b), prepared following the general requirements of the Intera DGR Project Quality Plan (Intera Engineering Ltd., 2009).

2 Standard Operating Procedures

The test program was carried out at the CANMET-MMSL's Rock Mechanics test facility located in Bells Corners. The Rock Mechanics test facility is managed by the Ground Control Program. The test facility is an ISO 17025 (International Standards Organization) accredited testing laboratory. Standard Operating Procedures (SOPs) that form part of the facility's accredited test procedures were selected for this project. The Standard Operating Procedures used for this test program were:

- SOP-T 2100 Specimen Preparation, Standardization and Dimensional Tolerance Verification,
- SOP-T 2103 Compressional P-Wave Velocity Test,
- SOP-T 2112 Uniaxial Compressive Strength Test with Servo Computer Control Press, and
- SOP-T 2113 Uniaxial Elastic Moduli and Poisson's Ratio Test with Servo Computer Control Press.

3 Specimens

Upon receipt the specimens were stored in an environmental chamber to minimize the loss or gain of moisture from. The 75-76 mm diameter specimens originated from boreholes DGR-3 and DGR-4. The total number of specimens received and tested comprised 11 UCS tests.

The procedure for the preparation of a cylindrical specimen conforms to the ASTM D4543 standard (ASTM, 2008a) and CANMET-MMSL SOP-T 2100. The wet specimens were jacketed with heat-shrink tubing prior to sample preparation, to minimize the loss or gain of water. The end surfaces of specimens were ground flat to within 0.025 mm, parallel to each other to within 0.025 mm, and perpendicular to the longitudinal axis of the specimen to within 0.25 degrees as determined using a gauge plate and dial gauge.

Specimen lengths were determined to the nearest 0.025 mm. Specimen diameters were measured to the nearest 0.025 mm by averaging three measurements taken at the mid height of the specimens spaced 120° apart. The average diameter was used for calculating the cross-sectional area. The volumes of the specimens were calculated from the length and diameter measurements. The weights of the specimens were determined to the nearest 0.01 g and the densities of the specimens were computed to the nearest 0.001 Mg/m³. The borehole, depth, dimensions, bulk density, and geologic formation of each tested specimen, are listed in Table A-1.

4 Test Apparatus and Procedures

4.1 Zero Pressure Velocity Tests

Zero pressure P-wave and S-wave velocities were measured for all the uniaxial specimens. The testing apparatus comprised a pulse generator, power amplifier, pulsing and sensing heads (transmitter and receiver) and oscilloscope. The P-wave and S-wave velocities were measured in accordance with SOP-T2103, and ASTM standard D2845, (ASTM, 2008b).

4.2 Uniaxial Compression Strength Tests

Compressive strength tests were conducted in a computer controlled, servo-hydraulic compression machine, consisting of a 2.22 MN rated load cell, load frame, hydraulic power supply, digital controller and test software. Three linear variable differential transformers (LVDTs) were arrayed around the specimen at 120 degree intervals for the measurement of axial deformations. A circumferential extensometer was used to measure specimen circumferential deformation.

The UCS test specimens were loaded in stress control to imminent failure at a rate of 0.75 MPa/s in accordance with ASTM standard D7012, (ASTM, 2007). Data were scanned every second and stored digitally in engineering units. Time, axial load, axial strain and diametric strain were recorded during each test. The specimens were photographed before and after testing.

5 Analysis of Data

5.1 Zero Pressure Velocity Tests

The P-wave (compressive) and S-wave (shear) velocities were determined by dividing the specimen length by the wave travel time through the specimen. The dynamic properties were then calculated using the following equations:

Dynamic Young's Modulus

$$E_d = \frac{\rho V_s^2 (3V_p^2 - 4V_s^2)}{V_p^2 - V_s^2} \quad (1)$$

where: E_d = dynamic Young's modulus
 V_s = shear wave velocity
 V_p = compressive wave velocity
 ρ = density

Dynamic Shear Modulus

$$G_d = \rho V_s^2 \quad (2)$$

where: G_d = dynamic shear modulus
 V_s = shear wave velocity
 ρ = density

Poisson's Ratio (based on velocity data)

$$\nu_d = \frac{V_p^2 - 2V_s^2}{2(V_p^2 - V_s^2)} \quad (3)$$

where: ν_d = Poisson's Ratio
 V_s = shear wave velocity
 V_p = compressive wave velocity

The velocity measurements and calculated dynamic properties are contained in Table A-2.

5.2 Uniaxial Compression Strength Tests

Data obtained from the uniaxial compression tests included the axial stress (σ), the axial strain (ϵ_a) and the circumferential strain (ϵ_c). Strains were calculated using extensometer data. Stress and strain were calculated as follows:

Axial Stress

$$\sigma = \frac{P}{A_0} \quad (4)$$

where: σ = axial stress
 P = applied axial load
 A_0 = initial specimen cross-sectional area

Axial Strain

$$\epsilon_a = \frac{\Delta l}{l_0} \quad (5)$$

where: ϵ_a = axial strain
 Δl = change in length of specimen
 l_0 = initial length of specimen

Circumferential Strain

$$\varepsilon_c = \frac{\Delta d}{d_0} \quad (6)$$

where: ε_c = circumferential strain
 Δd = change in circumference of specimen
 d_0 = initial circumference of specimen

Volumetric Strain

$$\varepsilon_v = \varepsilon_a + 2\varepsilon_c \quad (7)$$

where: ε_v = volumetric strain
 ε_a = axial strain
 ε_c = circumferential strain

Ultimate uniaxial compressive strength σ_c , tangent Young's modulus of elasticity E, (calculated at 0.4 σ_c) and the Poisson's Ratio ν , were established in each uniaxial test case as per ASTM Standard D7012, (ASTM, 2007) using load cell, extensometer and strain gauge data. These values were calculated as follows:

Ultimate Uniaxial Compressive Strength

$$\sigma_c = \frac{P_c}{A_0} \quad (8)$$

where: σ_c = ultimate uniaxial compressive strength
 P = axial load at failure
 A_0 = initial specimen cross-sectional area

Young's Modulus of Elasticity

$$E = \frac{\sigma_{40}}{\varepsilon_{40}} \quad (9)$$

where: E = tangent Young's Modulus at 40% of peak strength
 σ_{40} = tangent stress at 40% of peak strength
 ε_{40} = tangent strain at 40% of peak strength

Poisson's Ratio

$$\nu = \frac{E_{axial}}{E_{lateral}} \quad (10)$$

where: ν = Poisson's Ratio
 E_{axial} = slope of axial stress-strain curve at 40% of peak strength
 $E_{lateral}$ = slope of lateral stress-strain curve at 40% of peak strength

The ultimate uniaxial compressive strength, peak strain, Young’s Modulus and Poisson’s Ratio values are contained in Table A-3. Specimen stress-strain curves are contained in Appendix B. The graphs display stress-strain data calculated using extensometers.

Crack damage stress σ_{cd} , is the stress level where the ϵ_v - ϵ_a curve reaches a maximum and starts to reverse in direction, indicating dilation due to the formation and growth of unstable cracks. Progressive fracturing failure process starts above σ_{cd} leading to the failure of the rock. Crack damage stress and crack initiation stress levels are contained in Table A-3. Volumetric strain and crack volumetric strain curves are displayed in Appendix B. Appendix C contains photographs of the specimens before and after testing.

Crack initiation stress σ_{ci} , is the stress level where the σ - ϵ_a and ϵ_{dv} - ϵ_a curves start to deviate from linear elastic behaviour, indicating the development and growth of stable cracks. The crack volumetric strain ϵ_{dv} is the difference between the volumetric strain ϵ_v observed in the test and the elastic volumetric strain ϵ_{ev} calculated by assuming ideal linear elastic behaviour throughout the test. The value of σ_{ci} , was derived from the plot of the ϵ_{dv} - ϵ_a curve.

Crack Volumetric Strain

$$\epsilon_{dv} = \epsilon_v - \epsilon_{ev} \tag{11}$$

where: ϵ_{dv} = crack volumetric strain
 ϵ_v = volumetric strain
 ϵ_{ev} = elastic volumetric strain

6 Results and Conclusions

This report has described the apparatus and procedures used to conduct various mechanical and dynamic property tests on rock units originating from sedimentary bedrock underlying the Bruce DGR site. The Uniaxial Compressive strengths separate the rock units into different strength categories according to ASTM guide D5878 (ASTM, 2008c), as follows:

Formation	Strength Category	UCS Range
Salina C Unit	weak-medium strong	(5-50 MPa)
Salina A1 Unit Carbonate	very strong	(100-250 MPa)
Salina A0 Unit	very strong	(100-250 MPa)
Guelph	medium strong-strong	(25-100 MPa)

Young’s modulus and Poisson’s ratio values were generally consistent with the strength determinations. Specimen DGR3-375.79 was tested with an open shale parting perpendicular to the axis. Specimen DGR3-276.82 failed prematurely along a pre-existing inclined weakness plane and the stress-strain data as shown in Figure B-1 of Appendix B have been adjusted. Volumetric strain and volumetric strain deviation calculations for sample DGR3-276.82 were based on modulus values calculated below a stress level of about 4 MPa due premature cracking and strain shifts.

7 Data Quality and Use

Data on geomechanical strength properties of DGR-3 and DGR-4 core described in this Technical Report are based on testing conducted in accordance with established and well defined ASTM testing procedures.

The results presented in this Technical Report are suitable for assessing the geomechanical strength properties of bedrock formations intersected by DGR-3 and DGR-4, and the development of descriptive geomechanical

models of the Bruce DGR site.

8 Disclaimer

Any determination and/or reference made in this report with respect to any specific commercial product, process or service by trade name, trademark, manufacturer or otherwise shall be considered to be opinion; CANMET-MMSL makes no, and does not intend to make any, representations or implied warranties of merchantability or fitness for a particular purpose nor is it intended to endorse, recommend or favour any specific commercial product, process or service. The views and opinions of authors expressed herein do not necessarily state or reflect those of CANMET-MMSL and may not be used for advertising or product endorsement purposes.

9 References

ASTM, 2008a. Designation D4543: Standard Practices for Preparing Rock Core as Cylindrical Test Specimens and Verifying Conformance to Dimensional and Shape Tolerances, 2008 Annual Book of ASTM Standards, Section 4: Construction, Volume 04.08: Soil and Rock (I), ASTM International, West Conshohocken (PA), pp. 725-730.

ASTM, 2008b. Designation D2845: Standard Test Method for Laboratory Determination of Pulse Velocities and Ultrasonic Constants of Rock, 2008 Annual Book of ASTM Standards, Section 4: Construction, Volume 04.08: Soil and Rock (I), ASTM International, West Conshohocken (PA), pp. 303-308.

ASTM, 2008c. Designation D5878: Standard Guides for Using Rock-Mass Classification Systems for Engineering Purposes, 2007 Annual Book of ASTM Standards, Section 4: Construction, Volume 04.09: Soil and Rock (II), ASTM International, West Conshohocken (PA), pp. 330-359.

ASTM, 2007. Designation D7012: Standard Test Method for Compressive Strength and Elastic Moduli of Intact Rock Core Specimens under Varying States of Stress and Temperatures; 2007 Annual Book of ASTM Standards, Section 4: Construction, Volume 04.09: Soil and Rock (II), ASTM International, West Conshohocken (PA), pp. 1429-1436.

Intera Engineering Ltd., 2010. Technical Report: Laboratory Geomechanical Strength Testing of DGR-3 and DGR-4 Core, TR-08-24, Revision 1, June 18, Ottawa.

Intera Engineering Ltd., 2009. Project Quality Plan, DGR Site Characterization, Revision 4, August 14, Ottawa.

Intera Engineering Ltd., 2008a. Phase 2 Geoscientific Site Characterization Plan, OPG's Deep Geologic Repository for Low and Intermediate Level Waste, Report INTERA 06-219.50-Phase 2 GSCP-R0, OPG 00216-REP-03902-00006-R00, April, Ottawa.

Intera Engineering Ltd., 2008b. Test Plan for Laboratory Geomechanical Lab Testing of DGR-3 & DGR-4 Core, TP-08-12, Revision 1, July 25, Ottawa.

Intera Engineering Ltd., 2006. Geoscientific Site Characterization Plan, OPG's Deep Geologic Repository for Low and Intermediate Level Waste, Report INTERA 05-220-1, OPG 00216-REP-03902-00002-R00, April, Ottawa.

APPENDIX A

Data and Calculation Tables

Table A-1 Formations, Dimensions and Densities of Specimens

Formation	Depth (m)	Length (mm)	Diameter (mm)	Mass (g)	Density (Mg/m ³)
DGR-3					
Salina C Unit	276.82	168.17	75.50	1804.26	2.40
*Salina A1 Carbonate Unit	375.79	165.02	75.61	1991.09	2.69
Salina A0 Unit	385.05	168.83	75.66	2076.07	2.73
Guelph	389.67	168.83	75.16	1789.18	2.39
DGR-4					
Salina C Unit	253.26	168.81	74.07	1757.80	2.42
	259.30	168.86	75.02	1775.20	2.38
Salina A1 Carbonate Unit	363.10	168.66	75.04	1998.91	2.68
Salina A0 Unit	372.15	168.89	75.16	2108.72	2.81
	373.77	168.97	75.21	2021.32	2.69
Guelph	375.80	168.92	74.73	1859.39	2.51
	376.81	168.78	74.83	1865.71	2.51

*Shale Parting

Table A-2 Dynamic Elastic Constants of Specimens

Depth (m)	Length (mm)	P-wave time (μ s)	P-wave velocity (km/s)	S-wave time (μ s)	S-wave velocity (km/s)	E (GPa)	Shear modulus (GPa)	Poisson's ratio (ν)
DGR-3								
276.82	168.17	61.1	2.75	96.8	1.74	16.91	7.23	0.17
375.79	165.02	33.4	4.94	52.8	3.13	61.24	26.25	0.17
385.05	168.83	27.7	6.09	50.5	3.34	78.55	30.57	0.28
389.67	168.83	40.7	4.15	72.6	2.33	32.83	12.92	0.27
DGR-4								
253.26	168.81	53.9	3.13	85.8	1.97	21.97	9.36	0.17
259.30	168.86	59.2	2.85	92.8	1.82	18.22	7.87	0.16
363.10	168.66	58.7	2.87	100.0	1.69	18.86	7.62	0.24
372.15	168.89	27.7	6.10	49.5	3.41	83.35	32.76	0.27
373.77	168.97	28.9	5.85	52.8	3.20	70.94	27.58	0.29
375.80	168.92	38.3	4.41	64.6	2.61	42.18	17.16	0.23
376.81	168.78	36.6	4.61	61.8	2.73	46.12	18.75	0.23

Table A-3 Static Elastic Constants of Specimens

Depth	Ultimate uniaxial strength	Transducers					Comments
		Peak strain	E	Poisson's ratio	Crack damage stress	Crack Initiation stress	
(m)	(MPa)	(%)	(GPa)	(ν)	(σ_s =MPa)	(σ_d =MPa)	
DGR-3							
276.82	9.63	0.14	9.63	0.06	3.88	3.13	B, (VN)
375.79	118.54	0.35	46.47	0.18	105.48	46.88	A, (BD)
385.05	166.04	0.31	65.31	0.40	113.27	67.67	G
389.67	37.89	0.23	19.08	0.25	32.84	16.40	A
DGR-4							
253.26	26.01	0.34	8.65	0.28	16.30	10.14	G
259.30	25.07	0.28	9.19	0.18	25.07	10.43	G
363.10	114.87	0.44	32.86	0.14	102.38	45.90	A, (BD)
372.15	249.82	0.51	64.83	0.44	163.45	102.83	G
373.77	177.05	0.36	60.12	0.44	95.59	72.61	C
375.80	45.10	0.23	21.79	0.30	29.27	17.34	C
376.81	98.09	0.28	42.66	0.40	63.92	38.81	G

Note 1

Failure Modes:

- A axial splitting
- B shear (degrees)
- C multiple shear
- D Cone
- E Cone and A
- F Cone and B
- G Cone and C

Discontinuities:

- (BG) Bedding – regular layering of units or beds in sedimentary rocks
- (BD) Boundary – surface delineating different rock types or strength
- (CV) Cleavage – closely spaced parallel surfaces of fissility
- (CN) Contact – surface between two non sedimentary rock types
- (GS) Gneissosity – surface parallel to metamorphic lithological layering
- (SC) Schistosity – surface of easy splitting in metamorphic rocks defined by preferred orientation of minerals
- (VN) fracture in rock with less than 3cm of filling

APPENDIX B

Stress-Strain Curves of Tests

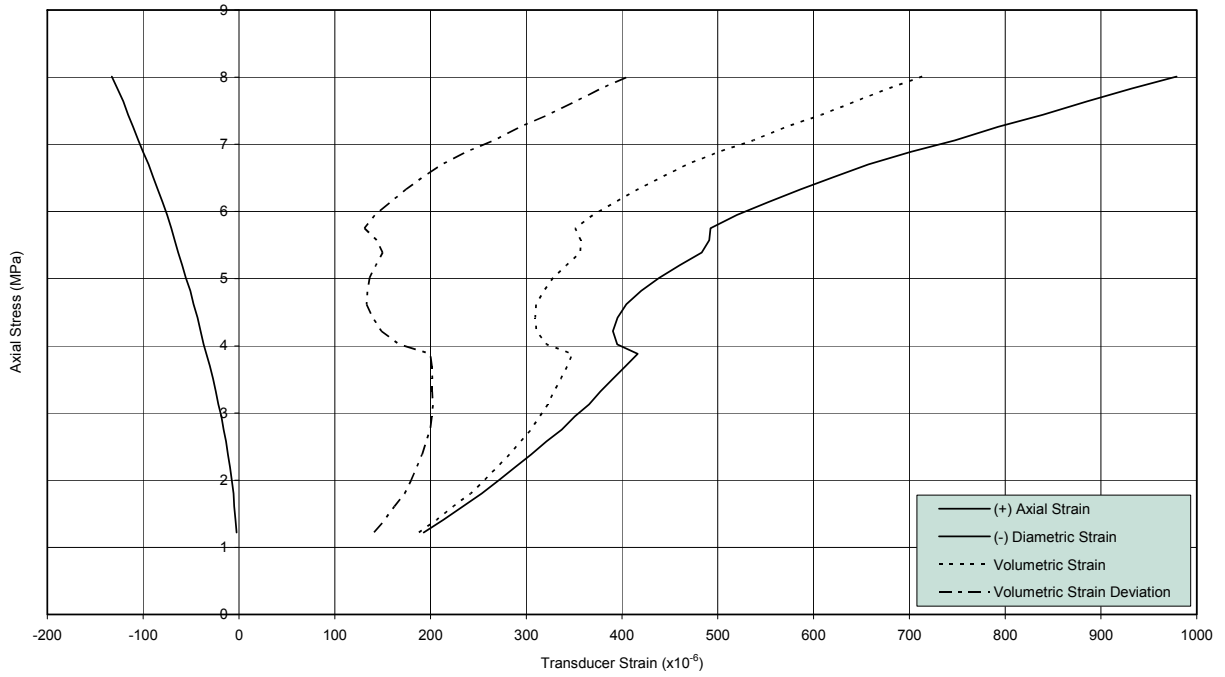


Figure B-1 UCS Specimen DGR-3, 276.82 m

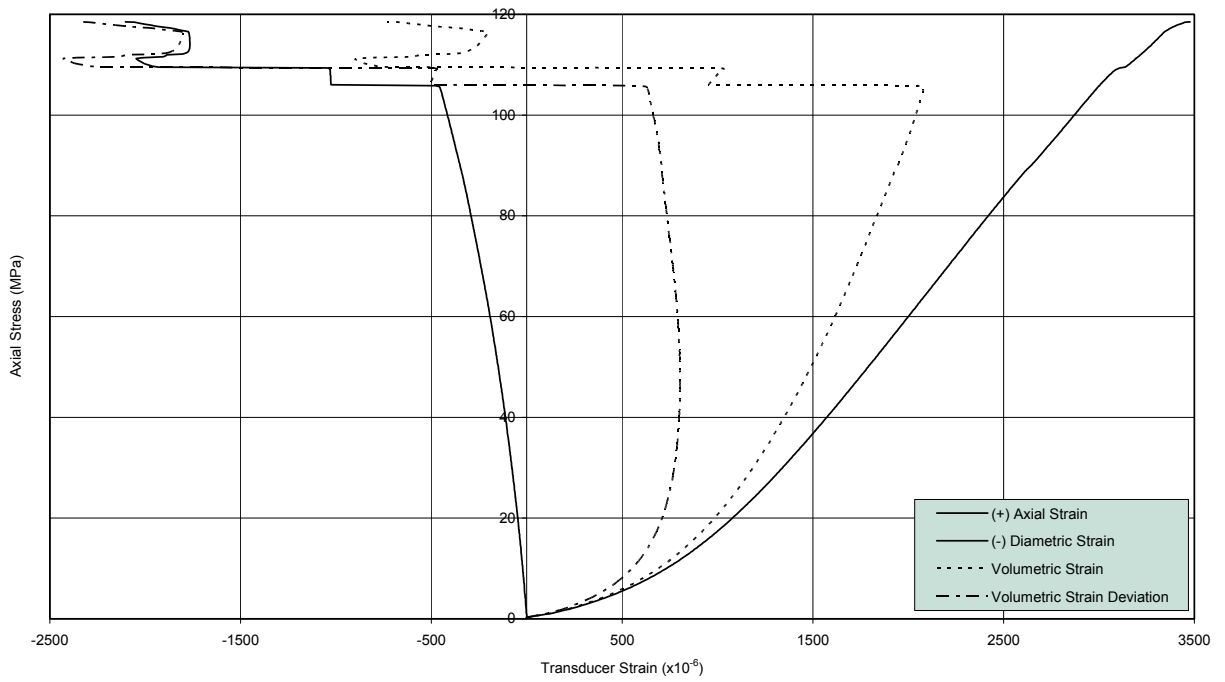


Figure B-2 UCS Specimen DGR-3, 375.79 m

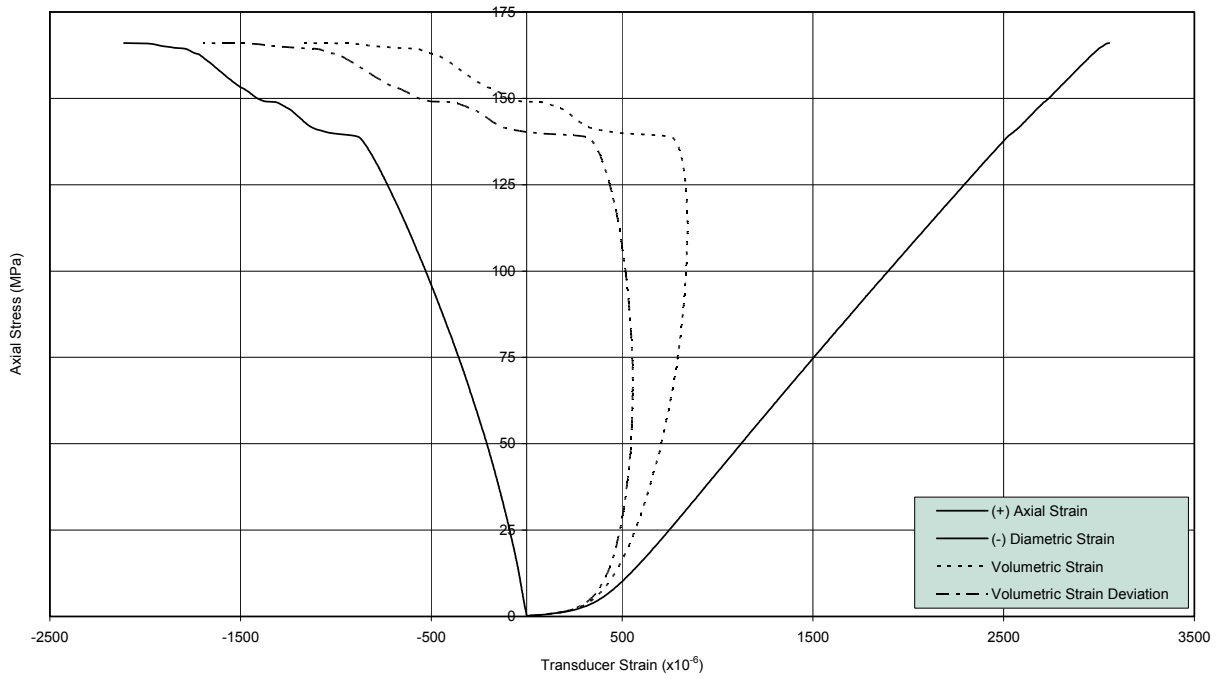


Figure B-3 UCS Specimen DGR-3, 385.05 m

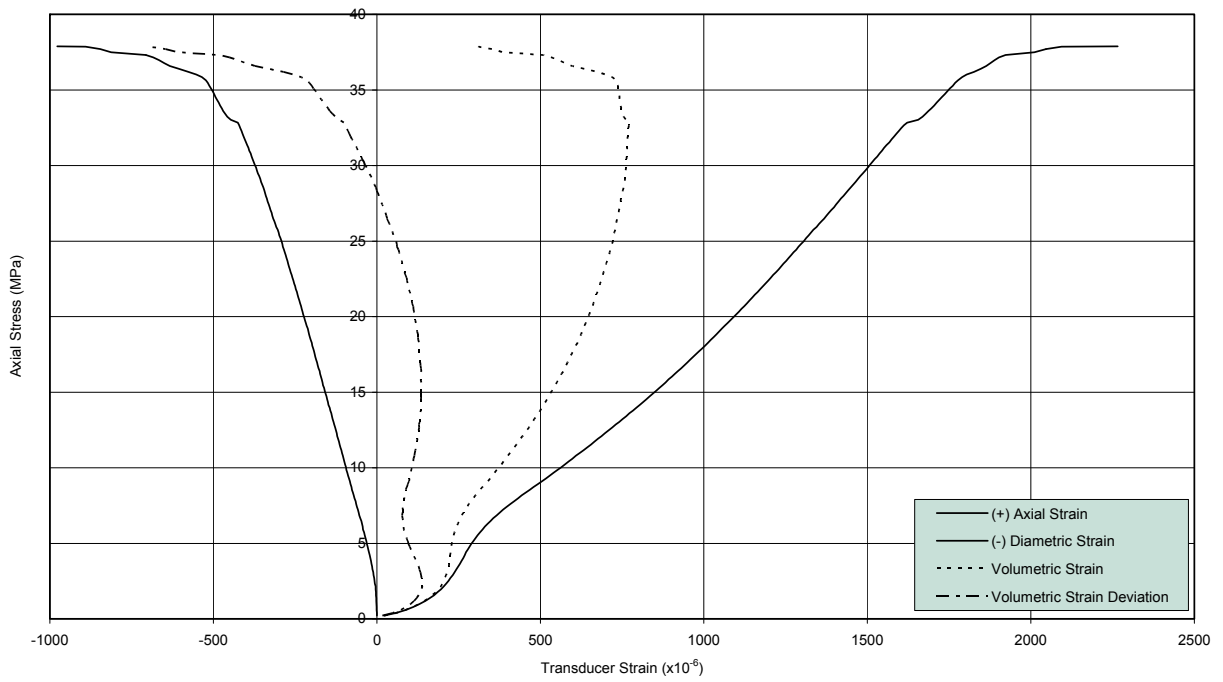


Figure B-4 UCS Specimen DGR-3, 389.67 m

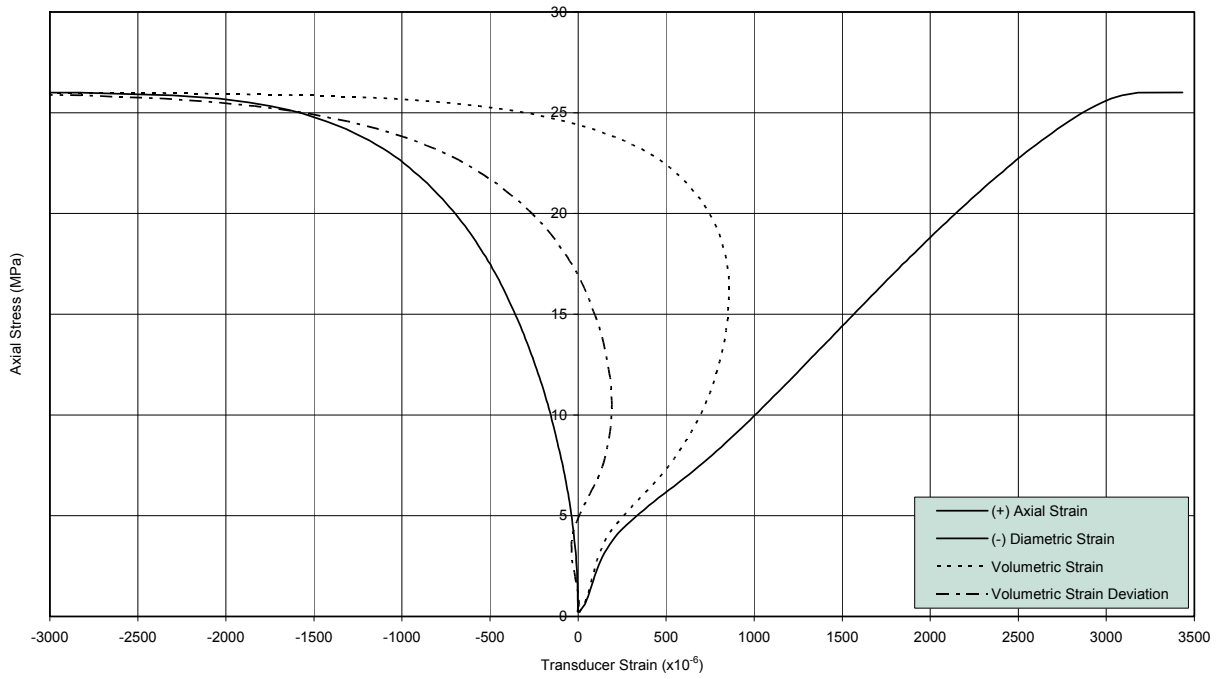


Figure B-5 UCS Specimen DGR-4, 253.26 m

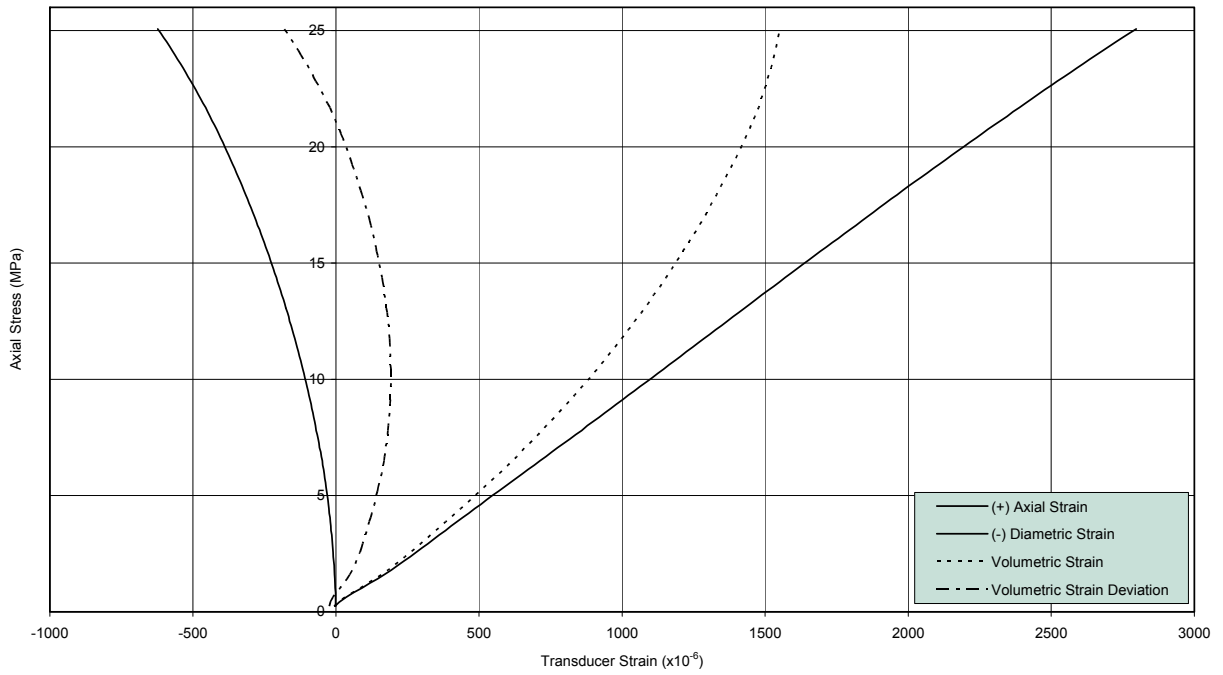


Figure B-6 UCS Specimen DGR-4, 259.30 m

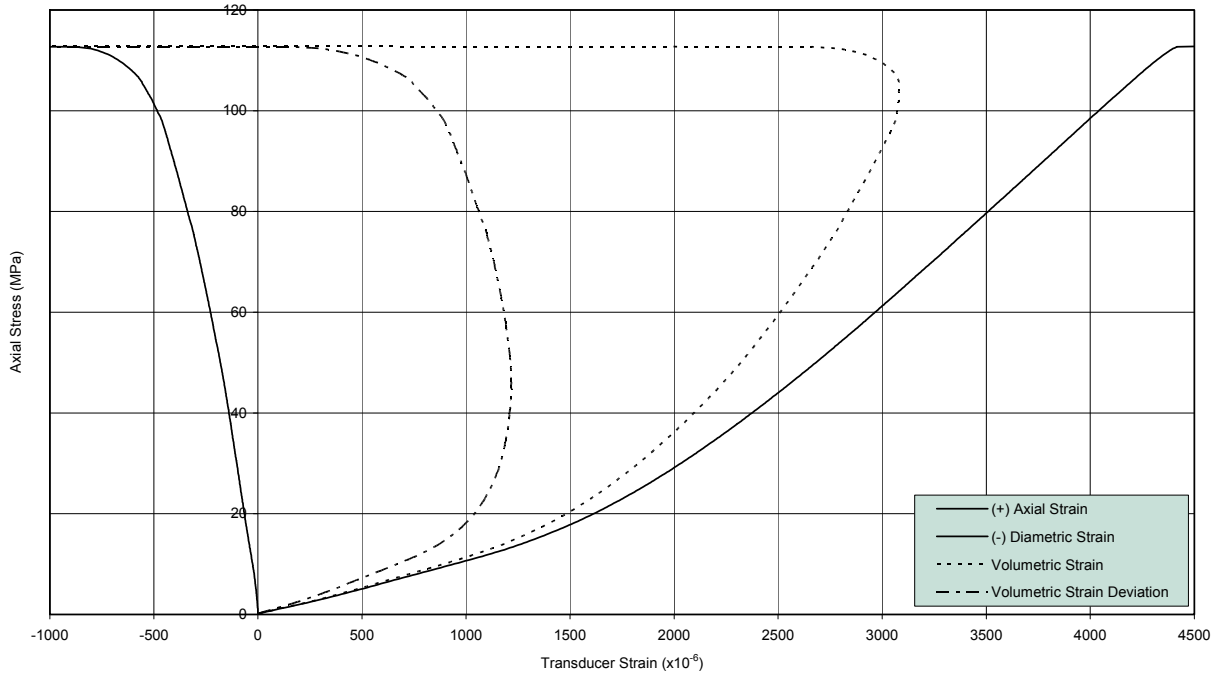


Figure B-7 UCS Specimen DGR-4, 363.10 m

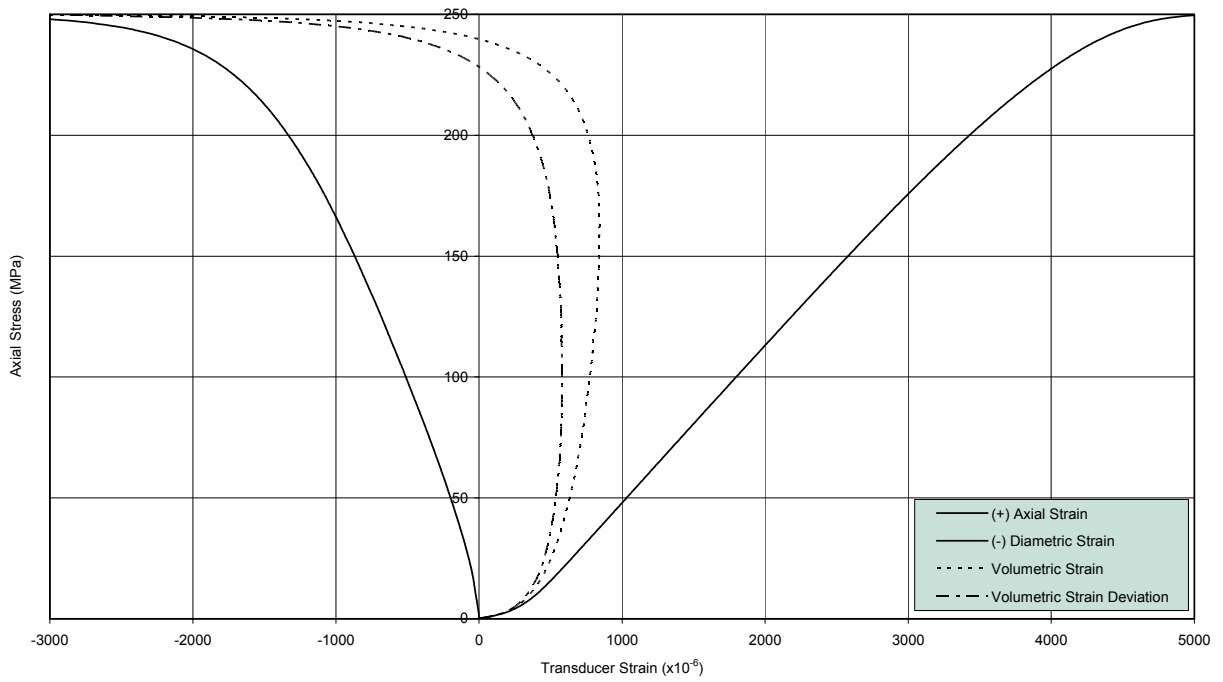


Figure B-8 UCS Specimen DGR-4, 372.15 m

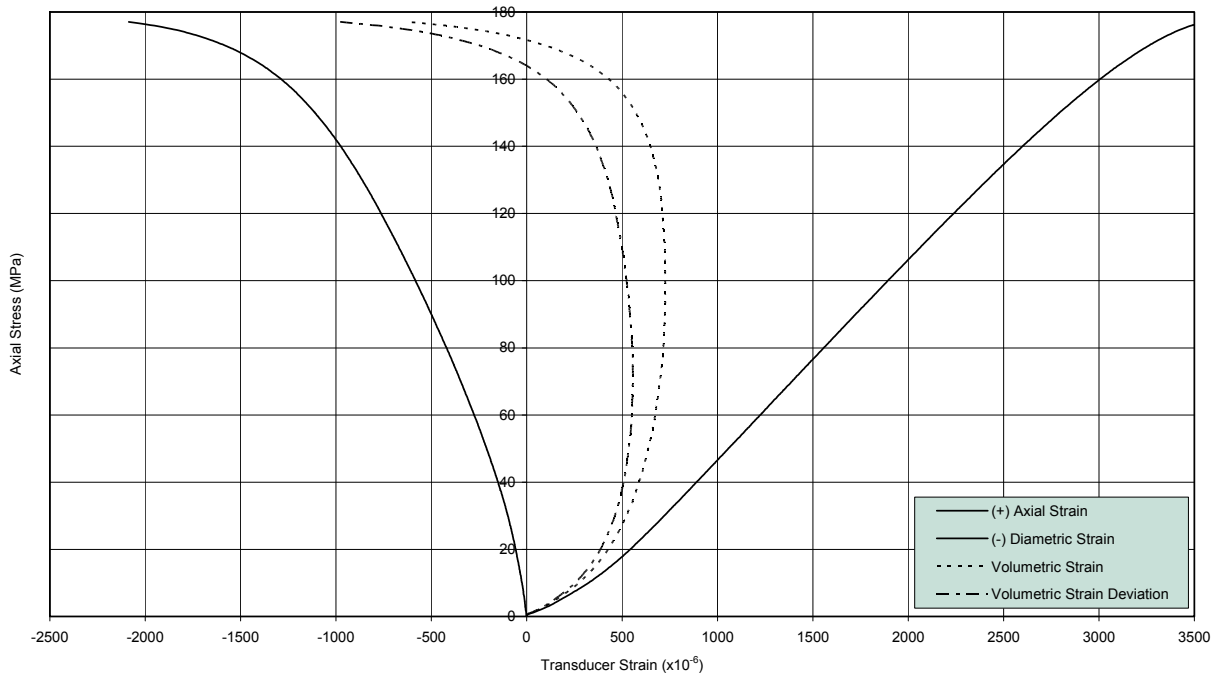


Figure B-9 UCS Specimen DGR-4, 373.77 m

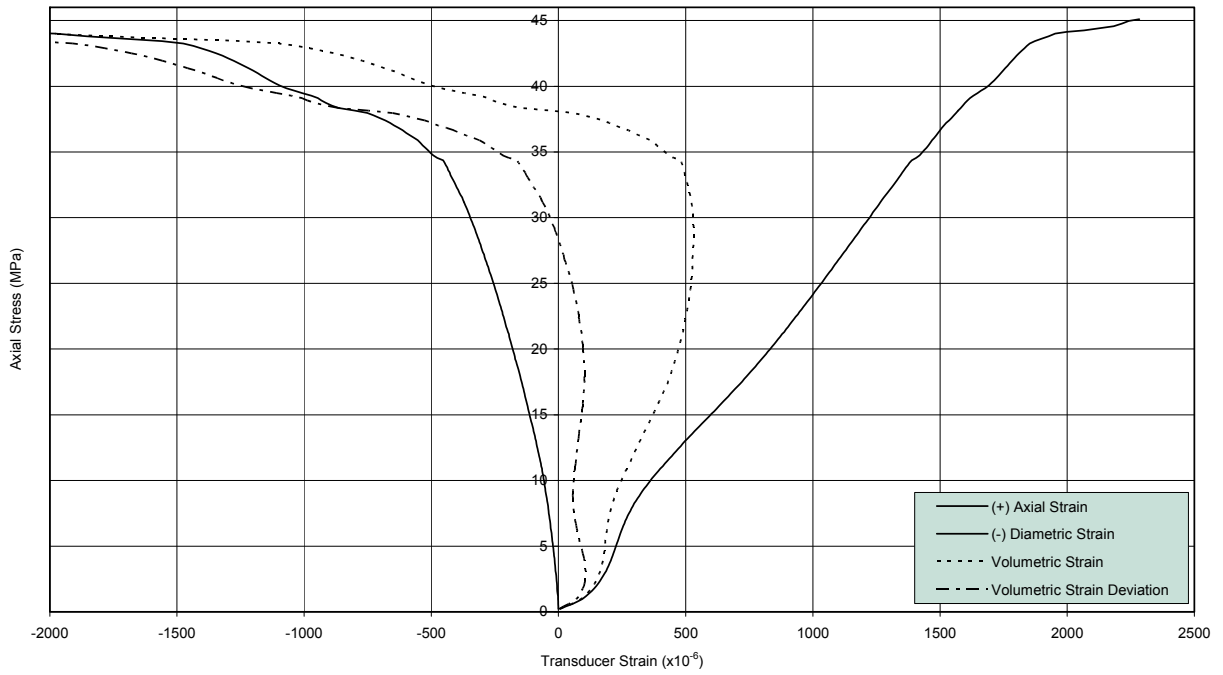


Figure B-10 UCS Specimen DGR-4, 375.80 m

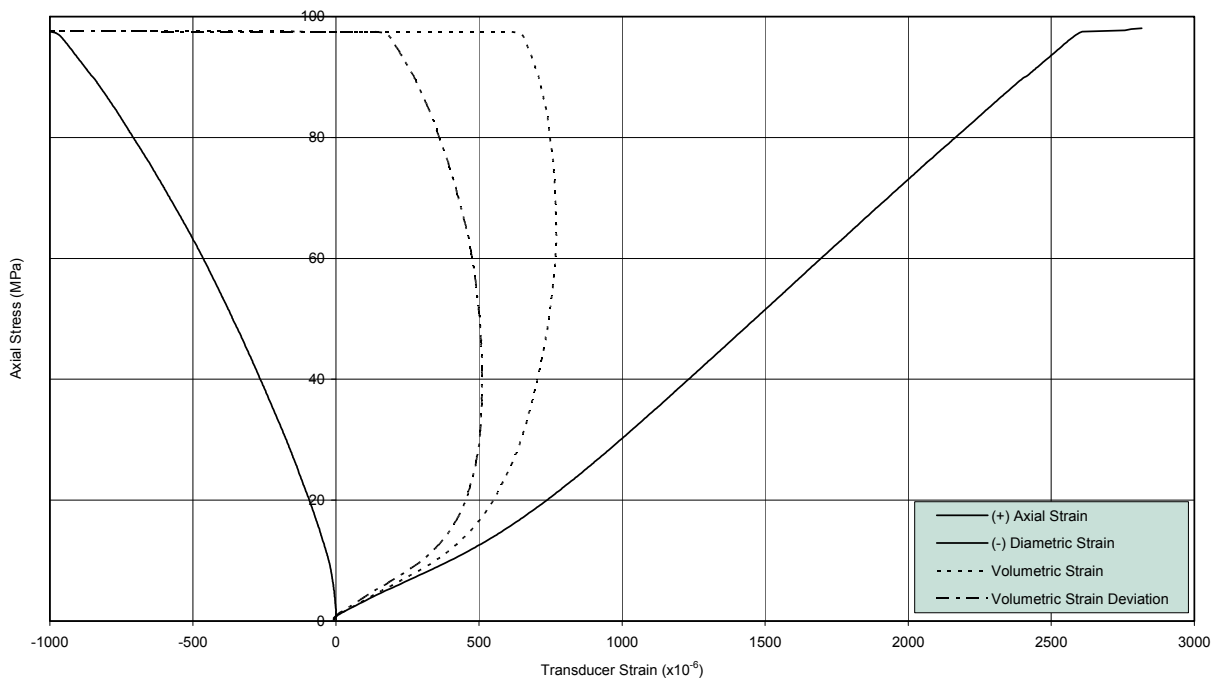


Figure B-11 UCS Specimen DGR-4, 376.81 m

APPENDIX C

Specimens Photographs (Before and After Tests)



Before



After

Figure C-1 UCS Specimen DGR-3, 276.82 m



Before



After

Figure C-2 UCS Specimen DGR-3, 375.79 m



Before



After

Figure C-3 UCS Specimen DGR-3, 385.05 m



Before



After

Figure C-4 UCS Specimen DGR-3. 389.67 m



Before



After

Figure C-5 UCS Specimen DGR-4, 253.26 m



Before



After

Figure C-6 UCS Specimen DGR-4, 259.30 m



Before

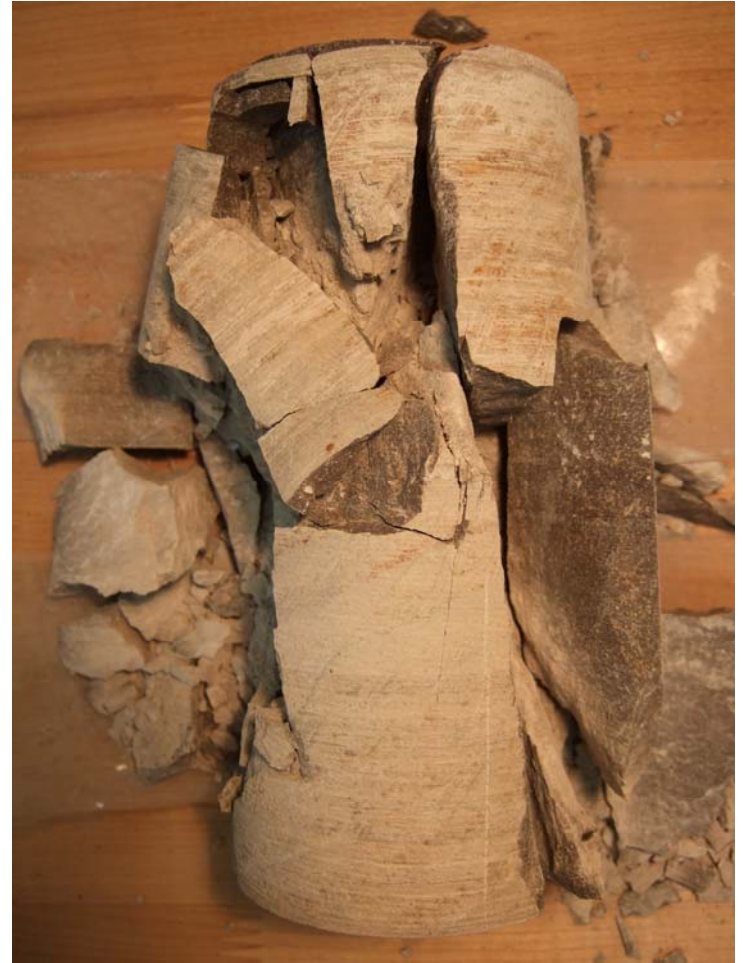


After

Figure C-7 UCS Specimen DGR-4, 363.10 m



Before

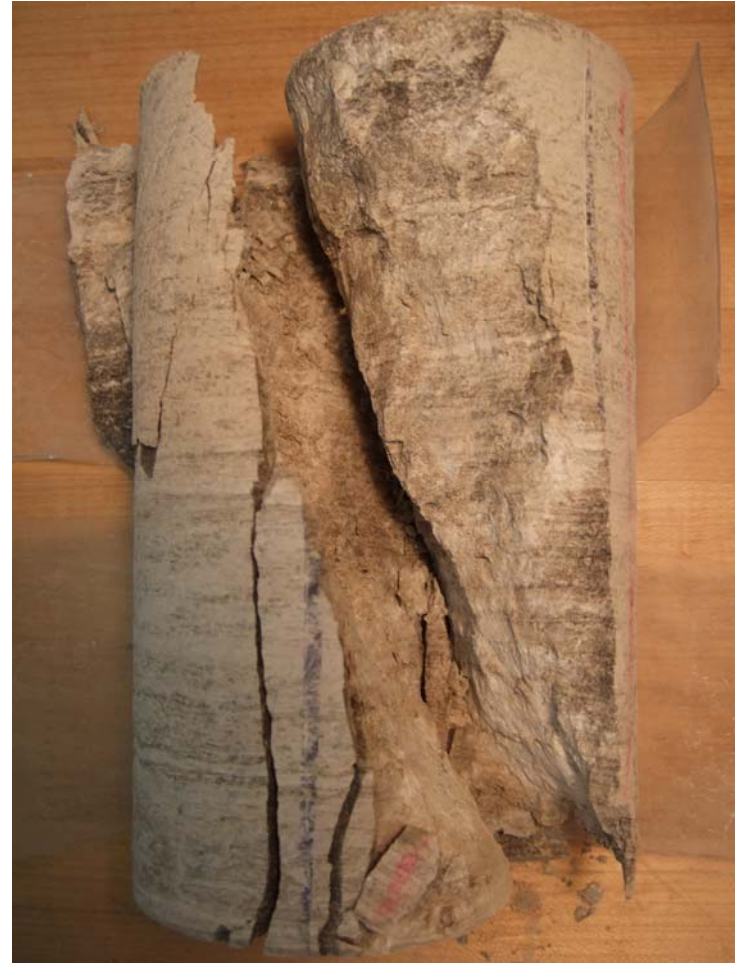


After

Figure C-8 UCS Specimen DGR-4, 372.15 m



Before



After

Figure C-9 UCS Specimen DGR-4, 373.77 m



Before



After

Figure C-10 UCS Specimen DGR-4, 375.80 m



Before



After

Figure C-11 UCS Specimen DGR-4, 376.81 m